

Intrinsic Viscosity of Polystyrene in Toluene-Supercritical Carbon Dioxide Mixtures

By Masamichi ONISHI,¹ Yo NAKAMURA,^{2,*} and Takashi NORISUYE¹

Intrinsic viscosities $[\eta]$ were determined for five polystyrene samples ranging in molecular weight M_w from 9.0×10^4 to 1.2×10^6 in toluene-supercritical carbon dioxide mixtures with different weight fractions of CO_2 (denoted as $w(\text{CO}_2)$) at 40°C in a pressure range $P = 7.0\text{--}10.0\text{ MPa}$ using a rolling-ball viscometer. For every sample $[\eta]$ was a gradually increasing function of P , indicating that the polystyrene coil expands with increasing P . At fixed P and $w(\text{CO}_2)$, the molecular weight dependence of $[\eta]$ was expressed in the form $[\eta] \propto M_w^a$. The exponent a remarkably changed with $w(\text{CO}_2)$ at constant P ; for example, it decreased from 0.68 (a good solvent value) to 0.42 (a poor solvent value below the theta point where $a = 0.5$) with an increase in $w(\text{CO}_2)$ from 15 to 31% at $P = 7.0\text{ MPa}$. The solvent goodness was quantified in terms of the binary-cluster integral determined by analyzing the $[\eta]$ data according to the two-parameter theory.

KEY WORDS: Intrinsic Viscosity / High Pressure / Supercritical Liquid / Carbon Dioxide / Excluded-Volume Effect / Binary-Cluster Integral /

Supercritical carbon dioxide (critical temperature 31.1°C and pressure 7.38 MPa) is known to be compatible with many organic solvents. Such mixtures, in which polymer solubility is controllable by changing the pressure and the solvent composition,^{1–3} have possible applications to separation or blending of chemically different polymers and molecular weight fractionation of homopolymers.^{4,5} For the purpose of industrial processing, the dependence of viscosity η on temperature, pressure, and solvent composition was investigated for polymer + organic solvent + supercritical CO_2 systems.^{6,7} Most of these studies are, however, limited to rather high polymer concentrations (above 1 wt %) and fixed molecular weights M , and none of them discusses the effect of polymer chain dimensions or related molecular properties on η ; η of polymer solutions increases with increasing chain dimensions.

The intrinsic viscosity $[\eta]$ of a polymer coil (*i.e.*, a long flexible chain) is a basic molecular property related closely to the chain dimensions. It increases with an increase in M or solvent power (*i.e.*, the strength of intramolecular excluded volume in a term of polymer statistical mechanics), but such dependence of $[\eta]$ in an organic solvent containing supercritical CO_2 has not been explored despite the importance to our understanding of the effect of supercritical CO_2 on polymer solution properties.

In the present work, we determine $[\eta]$ for polystyrene (PS) samples in toluene-supercritical CO_2 mixtures as functions of molecular weight, solvent composition, and pressure higher than the boundary between one liquid phase and liquid-gas two phase regions.⁴ The relation between the extent of chain expansion and the solvent condition is discussed on the basis of excluded-volume theories.⁸

Table I. Results from light scattering measurements on polystyrene samples in toluene at 15°C

Sample	$M_w \times 10^{-4}$	M_w/M_n^a	$\langle S^2 \rangle^{1/2}/\text{nm}$	$A_2 \times 10^4 / \text{cm}^3 \text{mol g}^{-2}$
F-10	8.96	1.04	11.6	4.8
F-20	18.6	1.04	16.8	4.5
F-40	41.3	1.04	26.4	3.7
F-80	66.1	1.05	34.5	3.2
F-120	114	1.08	48.1	2.9
F-128	119	1.05	50.1	2.8

^aManufacturer's values

EXPERIMENTAL

Samples

Tosoh's standard PS samples F-10, F-20, F-40, F-80, F-120, and F-128 were once solved in benzene and freeze-dried before use. Weight-average molecular weights M_w for these samples in toluene at 15°C were determined by light scattering on a Fica-50 light scattering photometer. The results are summarized in Table I, along with the z-average radii of gyration $\langle S^2 \rangle^{1/2}$, second virial coefficients A_2 , and weight to number-average molecular weight ratios M_w/M_n .

Apparatus

Rolling-ball viscometers are often used for viscosity measurements of liquids under high pressure.^{9–13} Our apparatus including this type of viscometer is schematically shown in Figure 1. Liquid CO_2 from the tank (a) is compressed by the pump (c) (JASCO Co. Ltd. PU-980), which has a jacket cooled by circulated water from the cooling bath (b). The pressure inside the rolling-ball viscometer (f) placed in a temperature

¹Department of Macromolecular Science, Osaka University, 1-1 Machikaneyama-cho, Toyonaka 560-0043, Japan

²Department of Polymer Chemistry, Kyoto University, Katsura, Kyoto 615-8510, Japan

*To whom correspondence should be addressed (E-mail: yonaka@molsci.polym.kyoto-u.ac.jp).

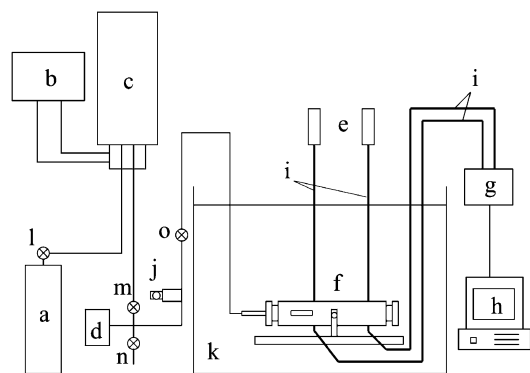


Figure 1. Schematic diagram of the apparatus constructed for viscosity measurements on polymer + organic solvent + supercritical CO₂ systems. a, CO₂ tank; b, water circulating bath; c, pump; d, pressure gauge; e, diode laser; f, rolling-ball viscometer; g, photo diode box; h, computer; i, optical fiber; j, safety valve; k, water bath; l-o, valves.

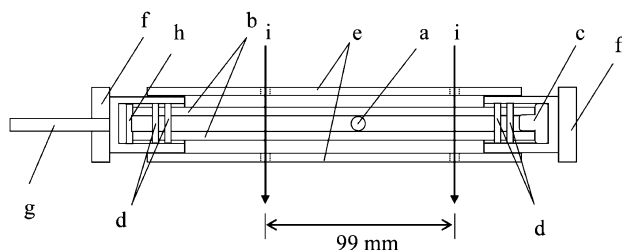


Figure 2. Schematic representation of rolling ball viscometer. a, glass ball; b, glass tube; c, Teflon stopper; d, gasket; e, stainless cylinder; f, stainless plug; g, CO₂ inlet; h, Teflon ring; i, laser light path.

controlled water bath (k) is monitored by the pressure gauge (d). Beams from the lasers (e) are incident to the viscometer through the optical fibers (i) and reach the photo diodes (g) after passing through the viscometer. The detected signal is processed by the computer (h).

Viscosity Measurement

The rolling-ball viscometer (*i.e.*, the cylindrical cell) is magnified in Figure 2. A glass ball (diameter 5.8 mm, TSC Co. Ltd., Kanagawa, Japan) is inserted in a Pyrex glass tube (inner diameter 6 mm, outer diameter 16 mm, and length 195 mm, Taiatsu Glass Co. Ltd., Tokyo, Japan). The cylinder is inclined at about 7° and the time required for the ball to move the distance between the two holes (separated by 99 mm in the middle of the cylindrical stainless jacket) is measured. The passage of the ball is optically detected at each hole where two glass fibers are inserted at the front and rear sides: one is for insertion of laser light and the other is for detection of the light by a photo diode at the other end of the fiber. The signals from the two photo diodes connected in series are processed by a computer to obtain the light intensity V (arbitrary units).

Since V abruptly decreases when the ball edge crosses the light path, two minimums appear for one hole as is shown in Figure 3. We take the time from the first to the third drop of V as the rolling time t . The specific viscosity η_{sp} and the relative viscosity η_r were determined from $(t - t_0)/t_0$ and t/t_0 ,

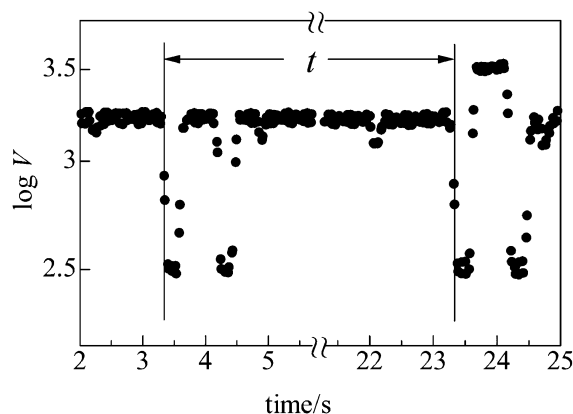


Figure 3. Example of photodiode signals.

respectively, where t_0 denotes the rolling time for the solvent at the same P and temperature. The Huggins (η_{sp}/c vs. c) and Fuoss-Mead ($\ln \eta_r/c$ vs. c) plots were used to extrapolate the measured viscosities to $c = 0$ (c is the polymer mass concentration).

Before high pressure experiments, measurements were made on toluene solutions of a PS sample ($M \sim 2 \times 10^5$) under atmospheric pressure. The $[\eta]$ value obtained agreed well with that determined by a conventional Ubbelohde-type capillary viscometer.

The procedure for the viscosity measurements on PS in toluene-supercritical CO₂ mixtures was as follows. A toluene solution of PS with a known amount and concentration was introduced into the cylindrical cell. After the apparatus had been set up, the viscometer was placed in the water bath controlled at 40 °C. Carbon dioxide was then introduced through the stainless tube until the inside pressure P reached a desired value (7.0, 8.5, or 10.0 MPa). The solution was stirred by tilting the cylinder to obtain a homogenous phase. This is consistent with the observation of Kim *et al.*⁴ on the same system ($M_w = 6.66 \times 10^5$, $w(\text{CO}_2) = 15.0\text{--}16.6\%$) that the solution becomes one liquid phase above *ca.* 4.5 MPa at 300 K. After the attainment of the temperature and pressure equilibrium, measurements were made. The weight fraction $w(\text{CO}_2)$ of CO₂ was calculated from the measured solution weight and P with the aid of the relation between the weight of CO₂ and P at 40 °C determined in advance for weighed pure toluene. The cylinder volume was found to be 7.4 cm³ from the known pressure-volume-temperature relation with the weight of pure CO₂ contained at 10.0 MPa and 25 °C. Figure 4 illustrates the Huggins and Fuoss-Mead plots for five PS samples at $w(\text{CO}_2) = 17\%$ and $P = 10.0$ MPa. The common intercept at $c = 0$ to the both plots gives $[\eta]$ for each sample.

RESULTS AND DISCUSSION

Pressure Dependence

Figure 5 shows $[\eta]$ data plotted against P for five PS samples in toluene-supercritical CO₂ mixtures with $w(\text{CO}_2) = 15, 16, \text{ and } 17$ wt % (at $P = 7.0, 8.5, \text{ and } 10.0$ MPa, respec-

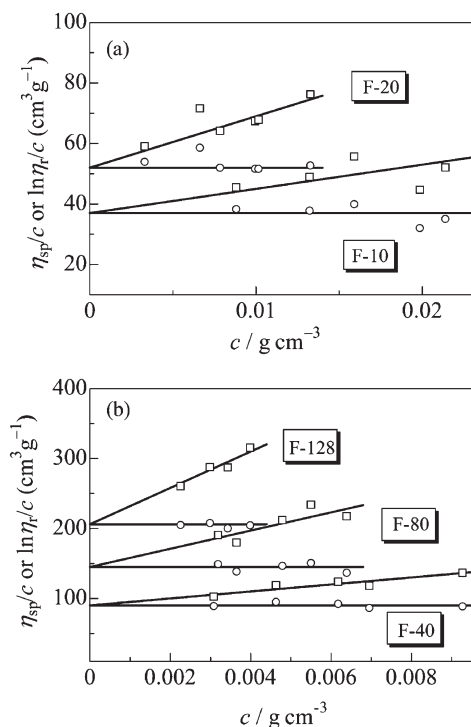


Figure 4. Huggins and Fuoss-Mead plots for the indicated PS samples at $w(\text{CO}_2) = 17\%$, $P = 10.0$ MPa, and 40°C .

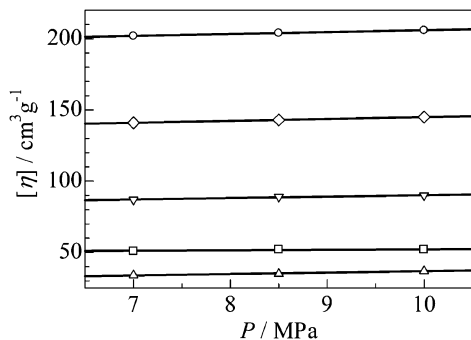


Figure 5. Plots of $[\eta]$ against P for PS samples in toluene-supercritical CO₂ with $w(\text{CO}_2) = 15$ ($P = 7.0$ MPa), 16 ($P = 8.5$ MPa), and 17 wt% ($P = 10.0$ MPa) at 40°C : triangles up, F-10; squares, F-20; triangles down, F-40; diamonds, F-80; circles, F-128.

tively). The line drawn for each sample rises very gradually with increasing P . Although this rise involves the effect of a small increase in $w(\text{CO}_2)$, the increase in CO₂ content lowers $[\eta]$ (see Figure 6). Thus, $[\eta]$ in toluene-supercritical CO₂ mixtures is an increasing function of P . In other words, the solvent power (or goodness) increases with increasing P . Similar pressure dependence of $[\eta]$ was observed for such polymer + pure solvent systems as poly(dimethylsiloxane) in cyclohexyl bromide¹¹ and PS in *tert*-butyl acetate.¹² Positive pressure dependence of solvent goodness was also observed by light scattering measurements of A_2 for PS in toluene^{14,15} and PS in 2-butanone.¹⁶ On the other hand, for PS in *trans*-decalin, $[\eta]$ ¹⁷ and A_2 ^{14,15} decreased with increasing P , exemplifying a lowering of solvent power with an increase in P .

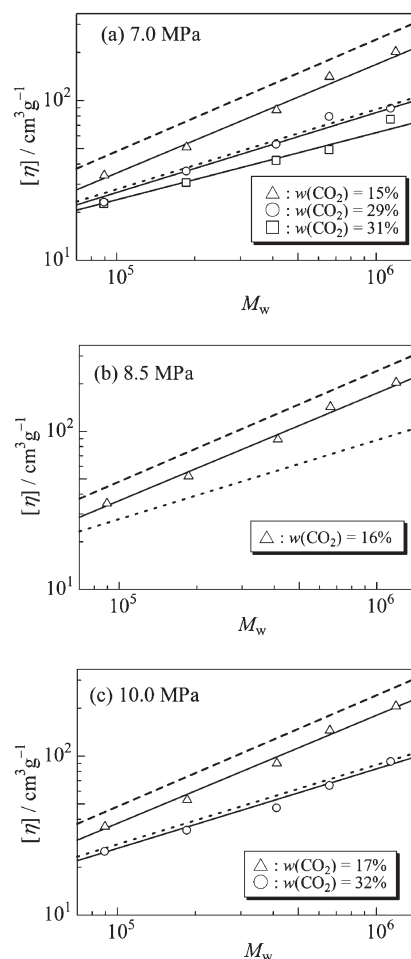


Figure 6. Molecular weight dependence of $[\eta]$ for PS in toluene-supercritical CO₂ mixtures with the indicated compositions at (a) $P = 7.0$, (b) 8.5 , and (c) 10.0 MPa, all at 40°C . Solid lines represent eqs 1–6. Dashed and dotted lines show the literature data for PS in toluene at 15°C ²¹ and in cyclohexane at 34.5°C ,²⁰ respectively.

It is known that the dielectric constant ϵ of most organic solvents increases with increasing P .¹⁸ Such an increase in ϵ of a solvent leads to either increase or decrease in solvent power depending on whether the difference in polarity between the solvent and the polymer diminishes or increases, as was observed for polymer + pure solvent systems. In our system, the increase in solvent power with increasing P may be interpreted as the result of the enhancing effect of increasing ϵ that surpasses the lowering effect of increasing CO₂ in toluene. Li *et al.*¹⁹ found the opposite tendency, *i.e.*, a decrease in $[\eta]$ with increasing P for PS ($M_w = 7.8 \times 10^4$) in toluene at 35°C under CO₂ atmosphere of $P < 4.2$ MPa. In their system, in which the polymer solution and the CO₂ gas phase coexist differing from our systems, ϵ may not significantly change with P , because the pressure is not very high. As is mentioned in their paper, the decrease in $[\eta]$ can be attributed primarily to the increase in CO₂ content in toluene with increasing P .

Molecular Weight Dependence

Figure 6 shows double-logarithmical plots of $[\eta]$ against M_w

for PS in toluene-supercritical CO₂ mixtures at different sets of $w(\text{CO}_2)$ and P . The indicated straight lines fitting the data points for the respective sets can be expressed by the following equations (all in units of $\text{cm}^3 \text{g}^{-1}$):

At $P = 7.0$ MPa,

$$[\eta] = 0.014 M_w^{0.68} \quad \text{for } w(\text{CO}_2) = 15\% \quad (1)$$

$$[\eta] = 0.084 M_w^{0.50} \quad \text{for } w(\text{CO}_2) = 29\% \quad (2)$$

$$[\eta] = 0.19 M_w^{0.42} \quad \text{for } w(\text{CO}_2) = 31\% \quad (3)$$

At $P = 8.5$ MPa,

$$[\eta] = 0.014_5 M_w^{0.68} \quad \text{for } w(\text{CO}_2) = 16\% \quad (4)$$

At $P = 10.0$ MPa,

$$[\eta] = 0.015 M_w^{0.68} \quad \text{for } w(\text{CO}_2) = 17\% \quad (5)$$

$$[\eta] = 0.083 M_w^{0.50} \quad \text{for } w(\text{CO}_2) = 32\% \quad (6)$$

The viscosity exponent decreases with increasing $w(\text{CO}_2)$, revealing that the solvent goodness remarkably lowers as the CO₂ content increases.

The exponent 0.5 in eqs 2 and 6 corresponds to the theta state for random coils, *i.e.*, for long flexible chains. The experimental data under the two solvent conditions (circles) are close to each other and also to the dotted line in Figure 6a or 6b, which represents the literature $[\eta]$ data for PS in cyclohexane (34.5 °C),²⁰ a theta solvent. Lechner and Schulz¹⁴ showed that the unperturbed dimension of PS in toluene and trans-decalin decreases when the solution pressure increased up to 75 MPa. In our system, however, such hydrostatic pressure effect was not observed, probably because P in our experiments is not as high as theirs.

Equations 1, 4, and 5 have a larger exponent 0.68, indicating that the polymer coil is expanded by excluded-volume effect. The solvent power is, however, lower than pure toluene because the $[\eta]$ data (triangles) are considerably below the dashed lines representing $[\eta]$ in toluene (15 °C).²¹ At $P = 7.0$ MPa and $w(\text{CO}_2) = 31\%$, the exponent 0.42 is much smaller than 0.5 (eq 3), implying that the solvent is very poor.

Binary-Cluster Integral

The binary-cluster integral β representing the strength of the excluded-volume interaction between a pair of segments (or repeating units) in a single polymer chain is the most basic parameter for the solvent power and related to the excluded-volume parameter z defined by⁸

$$z = (3/2\pi b^2)^{3/2} n^{1/2} \beta \quad (7)$$

Here, b is the segment length and n the segment number in the polymer chain. With the intrinsic viscosity $[\eta]_0$ in the unperturbed state taken as the reference state, $[\eta]$ in a perturbed state can be written as⁸

$$[\eta] = \alpha_\eta^3 [\eta]_0 \quad (8)$$

where the intrinsic-viscosity expansion factor α_η^3 may be given by Barrett's equation²²

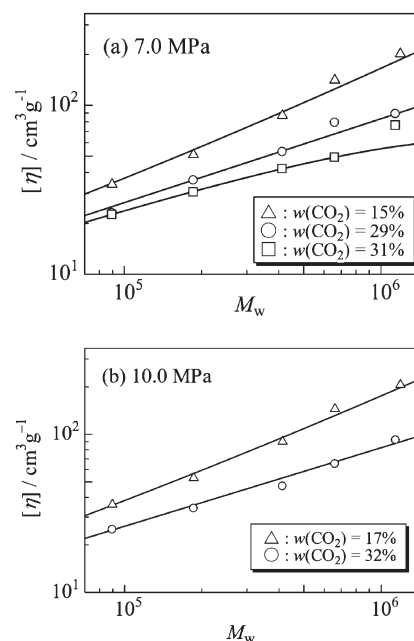


Figure 7. Comparison between observed (symbols) and calculated (solid lines) $[\eta]$ for PS samples in toluene-supercritical CO₂ mixtures with the indicated compositions at (a) $P = 7.0$ and (b) 10.0 MPa.

Table II. Binary-cluster integral for PS in toluene-supercritical CO₂ mixtures with different $w(\text{CO}_2)$ at 40 °C and at the indicated pressures

P/MPa	$w(\text{CO}_2)/\%$	β/nm^3
7.0	15	0.016
	29	0
	31	-0.0034
8.5	16	0.017
10.0	17	0.019
	32	0

$$\alpha_\eta^3 = (1 + 3.8z + 1.9z^2)^{0.3} \quad (9)$$

for $z > 0$. For $z < 0$ (*i.e.*, at $P = 7.0$ MPa and $w(\text{CO}_2) = 31\%$), we may use the first-order perturbation equation^{8,23}

$$\alpha_\eta^3 = 1 + 1.14z \quad (10)$$

Taking experimental $[\eta]$ for $w(\text{CO}_2) = 29\%$ at $P = 7.0$ MPa and $w(\text{CO}_2) = 32\%$ at $P = 10.0$ MPa as $[\eta]_0$, we may evaluate $[\eta]$ at these pressures and other $w(\text{CO}_2)$ from the above equations. The calculated solid lines in Figure 7a and 7b closely fit the data points for $P = 7.0$ and 10.0 MPa, respectively.

The β values determined from the fitting are summarized in Table II, where b in eq 7 was taken to be 0.72 nm (from the radius of gyration of PS in cyclohexane at 34.5 °C²⁴). This table includes the β value at $P = 8.5$ MPa and $w(\text{CO}_2) = 16\%$, similarly estimated with use of eq 2 for $[\eta]_0$. At almost the same CO₂ contents between 15 and 17%, β increases with raising P , reflecting the increase in solvent goodness.

CONCLUSIONS

We have determined intrinsic viscosities for five polystyrene samples of molecular weights 9.0×10^4 – 1.2×10^6 in toluene-supercritical CO₂ mixtures at 40 °C under high pressure (7–10 MPa). The results show that the increase in CO₂ content remarkably changes the solubility of polystyrene as indicated by a decrease in viscosity exponent a , for example, from 0.68 to 0.42 at $P = 7.0$ MPa. In case of $P = 7.0$ MPa and $w(\text{CO}_2) = 29\%$ or $P = 10.0$ MPa and $w(\text{CO}_2) = 32\%$, a becomes equal to the value 0.5 for the theta solvent system. Estimation of the binary-cluster integral from $[\eta]$ data based on the two-parameter theory substantiates that the solvent goodness in the present system is an increasing function of P .

Received: December 12, 2008

Accepted: February 13, 2009

Published: April 1, 2009

REFERENCES

1. M. A. McHugh and T. L. Guckes, *Macromolecules*, **18**, 674 (1985).
2. A. A. Kiamos and M. D. Donohue, *Macromolecules*, **27**, 357 (1994).
3. S. N. Joung, J.-U. Park, S. Y. Kim, and K.-P. Yoo, *J. Chem. Eng. Data*, **47**, 270 (2002).
4. S. Kim, Y.-S. Kim, and S.-B. Lee, *J. Supercrit. Fluids*, **13**, 99 (1998).
5. K. Liu and E. Kiran, *Polymer*, **49**, 1555 (2008).
6. S.-D. Yeo and E. Kiran, *Macromolecules*, **32**, 7325 (1999).
7. S.-D. Yeo and E. Kiran, *J. Appl. Polym. Sci.*, **75**, 306 (2000).
8. H. Yamakawa, "Modern Theory of Polymer Solutions," Harper & Row, New York, 1971.
9. R. M. Hubbard and G. G. Brown, *Ind. Eng. Chem., Anal. Ed.*, **15**, 212 (1943).
10. L. T. Carmichael and B. H. Sage, *Ind. Eng. Chem.*, **44**, 2728 (1952).
11. K. Kubota and K. Ogino, *Macromolecules*, **12**, 74 (1979).
12. J. R. Schmidt and B. A. Wolf, *Macromolecules*, **15**, 1192 (1982).
13. S. Sawamura, N. Takeuchi, K. Kitamura, and Y. Taniguchi, *Rev. Sci. Instrum.*, **61**, 871 (1990).
14. M. Lechner and G. V. Schulz, *Eur. Polym. J.*, **6**, 945 (1970).
15. G. V. Schulz and M. Lechner, *J. Polym. Sci., Part A-2*, **8**, 1885 (1970).
16. D. Gaeckle and D. Patterson, *Macromolecules*, **5**, 136 (1972).
17. K. Kubota and K. Ogino, *Polymer*, **20**, 175 (1979).
18. J. F. Skinner, E. L. Cussler, and R. M. Fuoss, *J. Phys. Chem.*, **72**, 1057 (1968).
19. D. Li, B. Han, Z. Liu, J. Liu, X. Zhang, S. Wang, X. Zhang, J. Wang, and B. Dong, *Macromolecules*, **34**, 2195 (2001).
20. Y. Einaga, Y. Miyaki, and H. Fujita, *J. Polym. Sci., Polym. Phys. Ed.*, **17**, 2103 (1979).
21. F. Abe, Y. Einaga, and H. Yamakawa, *Macromolecules*, **26**, 1891 (1993).
22. A. J. Barrett, *Macromolecules*, **17**, 1566 (1984).
23. J. Shimada and H. Yamakawa, *J. Polym. Sci., Polym. Phys. Ed.*, **16**, 1927 (1978).
24. Y. Miyaki, Y. Einaga, and H. Fujita, *Macromolecules*, **11**, 1180 (1978).